Supporting Information for:

The 2013 slab-wide Kamchatka earthquake sequence

B. Rousset[1], M. Campillo[2], N. M. Shapiro[2,3], A. Walpersdorf[2], N.

Titkov[4]and D. V. Chebrov[4]

[1]Institut Terre et Environnement de Strasbourg, UMR7063, Université de Strasbourg/EOST, CNRS, Strasbourg, France

[2]Institut des Sciences de la Terre, Université Grenoble Alpes, CNRS, Grenoble, France

[3]Schmidt Institute of the Physics of the Earth, Russian Academy of Sciences, Moscow, Russia

[4]Kamchatka Branch of the Geophysical Service, Russian Academy of Sciences, Petropavlovsk-Kamchatsky, Russia

Contents of this file

1. Sections 1 to 2

2. Table S1

3. Figures S1 to S10

Corresponding author: B. Rousset, Institut Terre et Environnement de Strasbourg, UMR7063, Université de Strasbourg/EOST, CNRS, Strasbourg, France. (baptiste.rousset@unistra.fr)

December 17, 2022, 1:47pm

1. GNSS Analysis

The GNSS data used in this study have been recorded by 10 continuous stations operated and maintained by the KBGS RAS. We have processed the time series for a 10-year period of time, from 2005 to 2015. Most of the sites have been active only a few years over the 10 years. The processing has been done with the GAMIT/GLOBK software (Herring et al., 2015). Non-tectonic signals such as ocean loading (Lyard et al., 2006), tidal and non-tidal atmospheric loading (Tregoning & van Dam, 2005) have been corrected. The variable tropospheric delay has been estimated using the Vienna tropospheric mapping function (Boehm et al., 2006) with its a priori meteorological data at each site, adjusting one zenith delay every two hours and two pairs of horizontal gradients per 24 hours. The local Kamchatka network has been completed with the 33 closest stations from the International GNSS Service (IGS) network, situated mainly on the Eurasian and North American plates. They were used to calculate position time series in the ITRF reference frame (Altamimi et al., 2012). Assuming negligible deformation between the Okhotsk micro-plate and the Eurasian plate, we estimated the interseismic velocity field with respect to the Eurasian plate, using eleven IGS stations situated on the stable plate (Fig. S6).

December 17, 2022, 1:47pm

2. Slip deficit and slip models

To model the transient deformation observed with GNSS observations in April 2013, we consider dislocations compatible with the subduction interface model slab 2.0 (Hayes et al., 2018) at a range of depths from the trench to the bottom of the slab at 600 km depth. We extended the geometry of the subduction interface slab 2.0 towards the seafloor surface by digitizing the trench location with the ETOPO1 bathymetry (Amante & Eakins, 2009). We also consider possible transient deformation on the coseismic plane of the M = 8.3 deep-focus earthquake published by (Ye et al., 2013). The Green's functions, $\mathbf{G}$, relating unit slip on each subduction interface or coseismic plane triangular patch to surface displacements are computed for a homogeneous, isotropic, elastic half-space (Thomas, 1993). The poisson's ratio ν is set to 0.25 and the shear modulus μ is the average of the PREM values (Dziewonski & Anderson, 1981) above the deepest patch of each model (depths < 60 km : $\mu = 43.10^9$ Pa ; depths < 200 km : $\mu = 48.10^9$ Pa ; depths < 400 km : $\mu = 56.10^9$ Pa ; depths < 650 km : $\mu = 69.10^9$ Pa). We have tested a range of forward and inverse models, both for slip and slip deficit. In the forward models, slip and slip deficit have been assumed to be homogeneous. To allow for possible lateral variations, we explored inverse models, for which we solve for the slip or slip deficit on each patch in the dip direction, $\mathbf{m}$, using the general least squares solution (Tarantola, 2005):

$$\mathbf{m} = \mathbf{m}_0 + \mathbf{C}_m \mathbf{G}^t (\mathbf{G} \mathbf{C}_m \mathbf{G}^t + \mathbf{C}_d)^{-1} (\mathbf{d} - \mathbf{G} \mathbf{m}_0), \tag{1}$$

where $\mathbf{m}_0$ is an a priori model (a null vector in this case). $\mathbf{d}$ includes the transient static offsets for the north and east components of the 10 stations used. $\mathbf{C}_d$ is a diagonal matrix including uncertainty variances (σ_d^2) associated with the transient offsets, where $\sigma_d = \sqrt{\left(\frac{\sigma_b}{\sqrt{N_b}}\right)^2 + \left(\frac{\sigma_a}{\sqrt{N_a}}\right)^2}$

models	RMSE slip (mm)	RMSE slip deficit (mm)
0-60	2.85	0.78
100-200	3.07	1.73
200-400	2.82	2.32
400-650	2.45	2.85
CP	2.40	2.84

Table S1.   Root mean square errors for slip and slip deficit for all the models tested. The numbers on the first column stand for the depth range of the models in km and CP for the coseismic plane from (Ye et al., 2013).

. σ_b and σ_a correspond to the standard deviation before and after the transient event. They are computed on time periods of durations $N_b = 80$ days and $N_a = 35$ days. The covariance between model parameters $\mathbf{C}_m$ is computed as $\mathbf{C}_m = \left(\frac{\sigma_m \lambda_0}{\lambda}\right)^2 \exp\left(\frac{\mathbf{x}}{\lambda}\right)$, where σ_m is an a priori standard deviation on the model parameters fixed to 0.1 m (Radiguet et al., 2011; Nocquet et al., 2014; Rousset et al., 2016). λ_0 is a scaling factor fixed at 50 km, λ is the correlation length and $\mathbf{x}$ is a vector with distances between pairs of patch centroids. λ is selected using a l-curve criterion (Fig. S7d). The RMS error for both slip and slip deficit inverse models is presented in Table S1. The best inverse models of each depth range on the subduction interface and the coseismic plane of (Ye et al., 2013) are shown in Fig. S7 and S8.
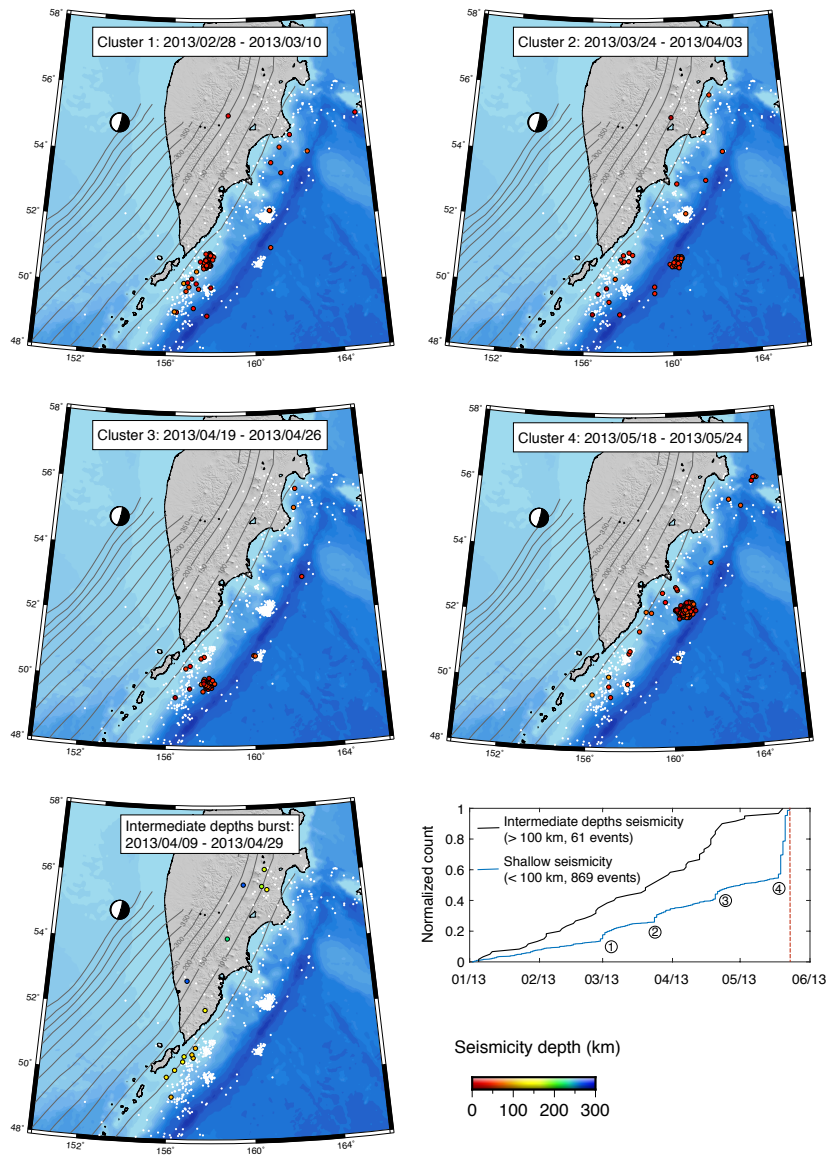
Figure S1.   Location of the seismic clusters and bursts. The top four panels indicate the location of earthquakes during the time periods indicated at the top, of the four shallow seismic clusters, between 0 and 100 km depth. The fifth map indicates the location of earthquakes during the intermediate depth seismicity burst, for depths > 100 km. The white dots show all the other earthquakes early 2013, before the Mw 8.3 mainshock on May 24 2013. The time series present the normalized cumulative number of events for depths < 100 km and > 100 km.

December 17, 2022, 1:47pm

Figure S2. Local magnitude (M$_l$) of individual events for the four shallow seismic clusters.
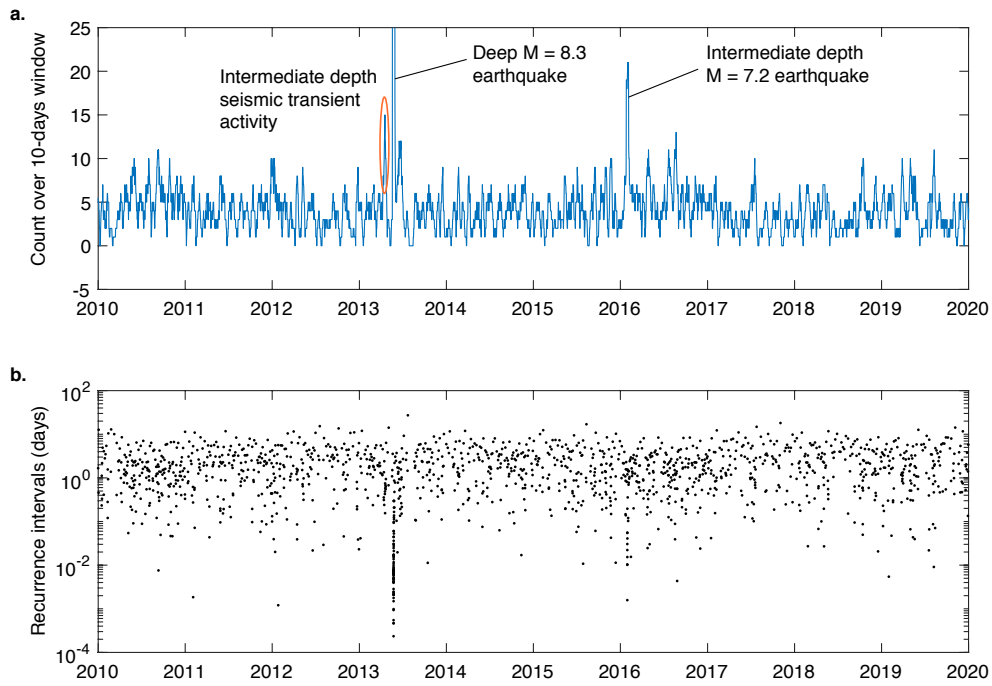
Figure S3. **Intermediate-depth and deep seismicity catalog (depths larger than 100 km) for a time period of 10 years.** (a) Count of the seismic events over 10-days sliding time windows. Earthquakes $M_l > 7.0$ are highlighted, as well as the seismic burst in April 2013. (b) Recurrence intervals of the seisms. Note the lineation in April 2013.
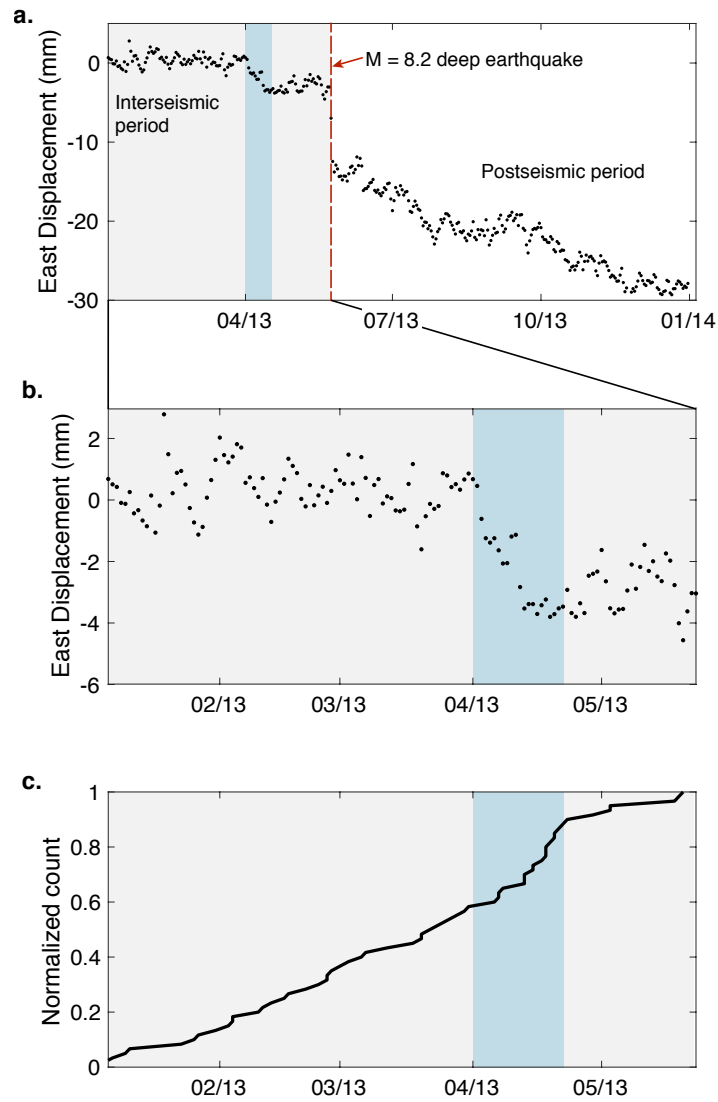
Figure S4.   2013 GNSS time series. (a) Averaged GNSS time series (East component) over the Kamchatka network during the full year 2013. (b) Zoom on the period of time before the Okhotsk M = 8.3 earthquake. (c) Cumulative number of earthquakes with depths > 100 km during the same period of time as in (b). The blue rectangles highlight the period of the transient event observed in both the GNSS time series and the intermediate depths earthquake count.
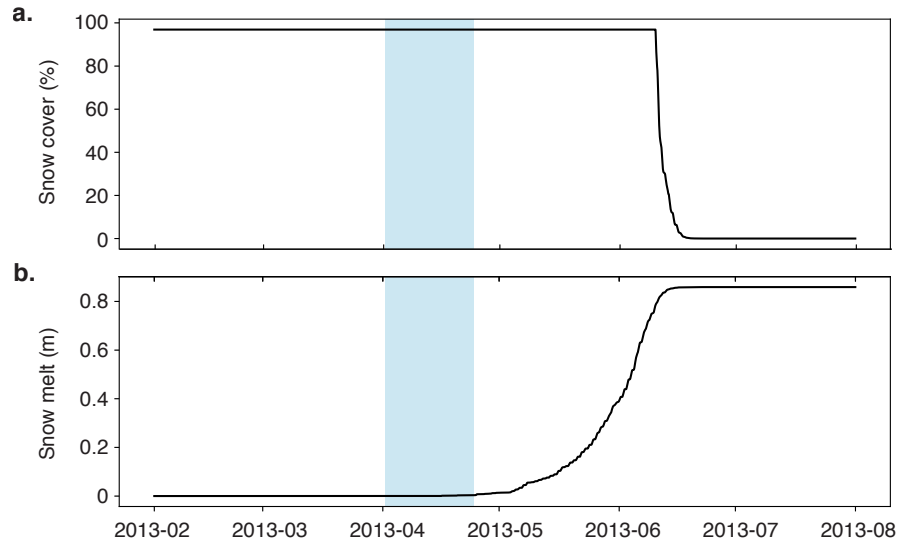
Figure S5.   Snow cover and snow melt in Kamchatka in 2013. (a) Snow cover at location 53.1°N 158.6°E, slightly north of Petropavlosk-Kamchatsky. (b) Snow melt at the same location. The ERA5 data shows similar timing for the snow melt over the whole Kamchatka peninsula. The light-blue rectangles indicate the timing of the transient deformation event observed with GNSS time series. The satellite ERA5 data can be found at https://cds.climate.copernicus.eu.
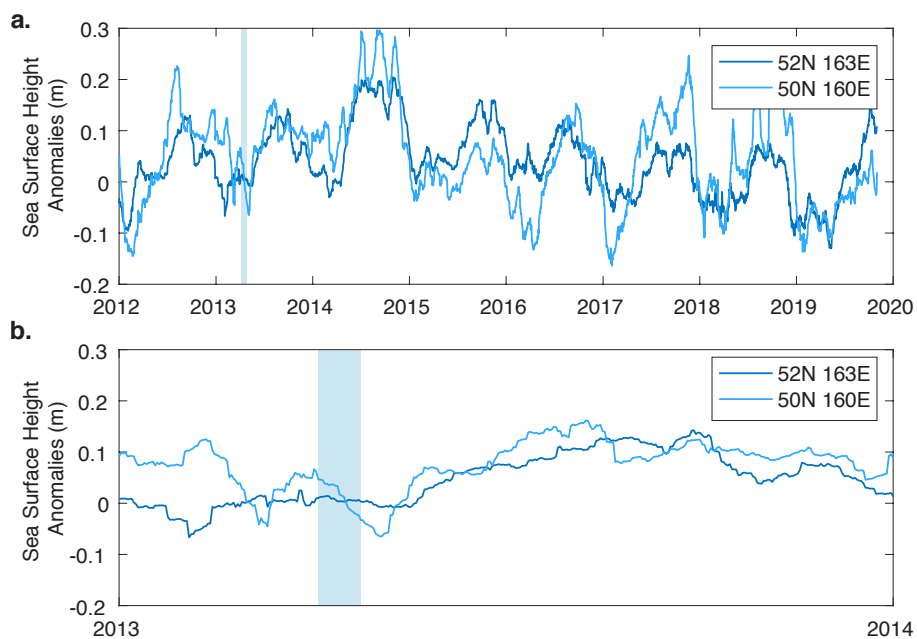
Figure S6.   Sea surface height anomalies (SSHA) east of the Kamchatka penin-sula in 2013. (a) SSHA from 2012 to 2020 at two locations above the Kamchatka trench. (b) Zoom on the year 2013. The light-blue rectangles indicate the timing of the transient deformation event observed with GNSS time series. The satellite altimetry data are available at: https://coastwatch.noaa.gov//erddap/griddap/noaacwBLENDEDSQsshDaily.html
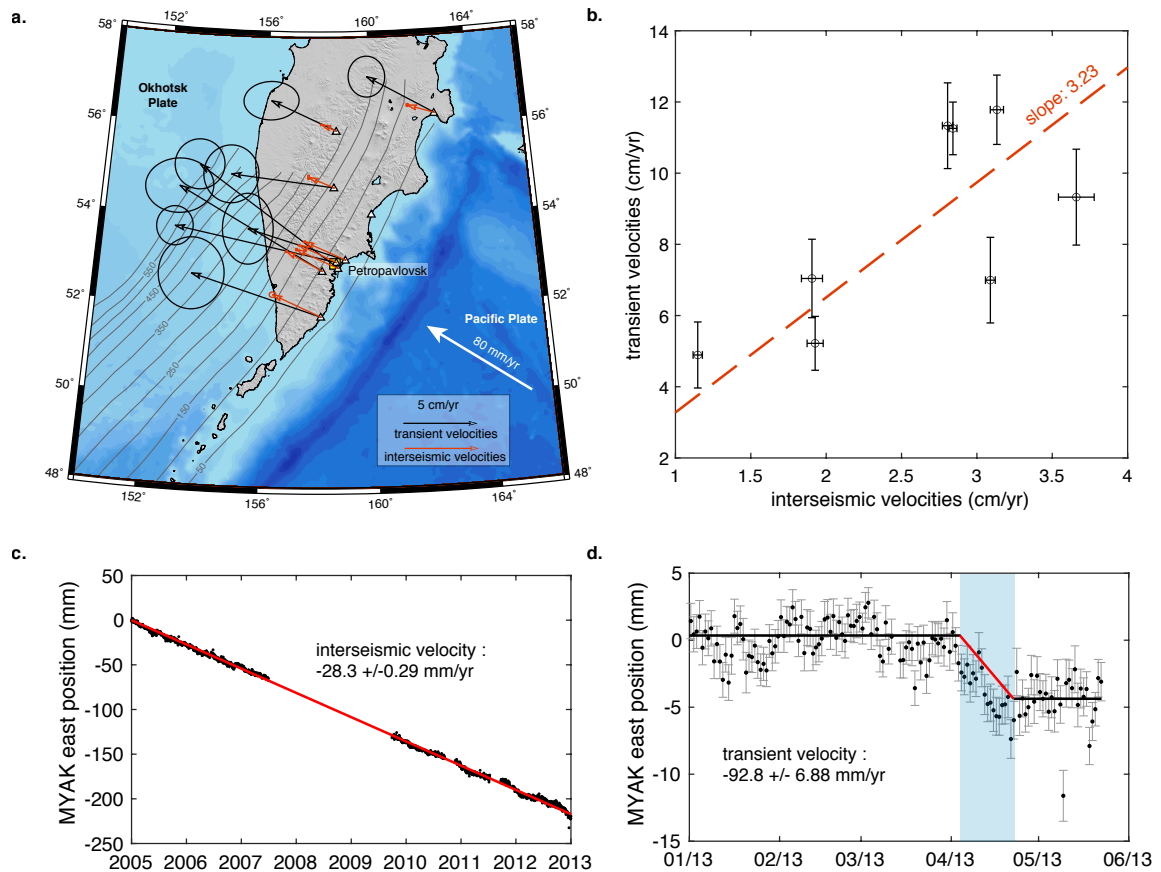
Figure S7. Transient velocities versus decadal interseismic velocities. (a) Map of the transient velocities in black and interseismic velocities in orange topped with 95% uncertainties. (b) Norm of the transient velocities compared with the norm of the interseismic velocities. The best linear fit and the corresponding slope are indicated. (c) Example of the east component of the position time series at site MYAK for the period 2005 to 2013 and the best linear fit in red which corresponds to the long-term interseismic velocities. (d) Example of the east component of the position time series at site MYAK for the first months of year 2013, before the Okhotsk earthquake. The black lines indicate the linear fits used to estimates the static offset of the transient deformation event. The red line shows the transient velocities that is computed by dividing the transient static offset by its duration (18 days).
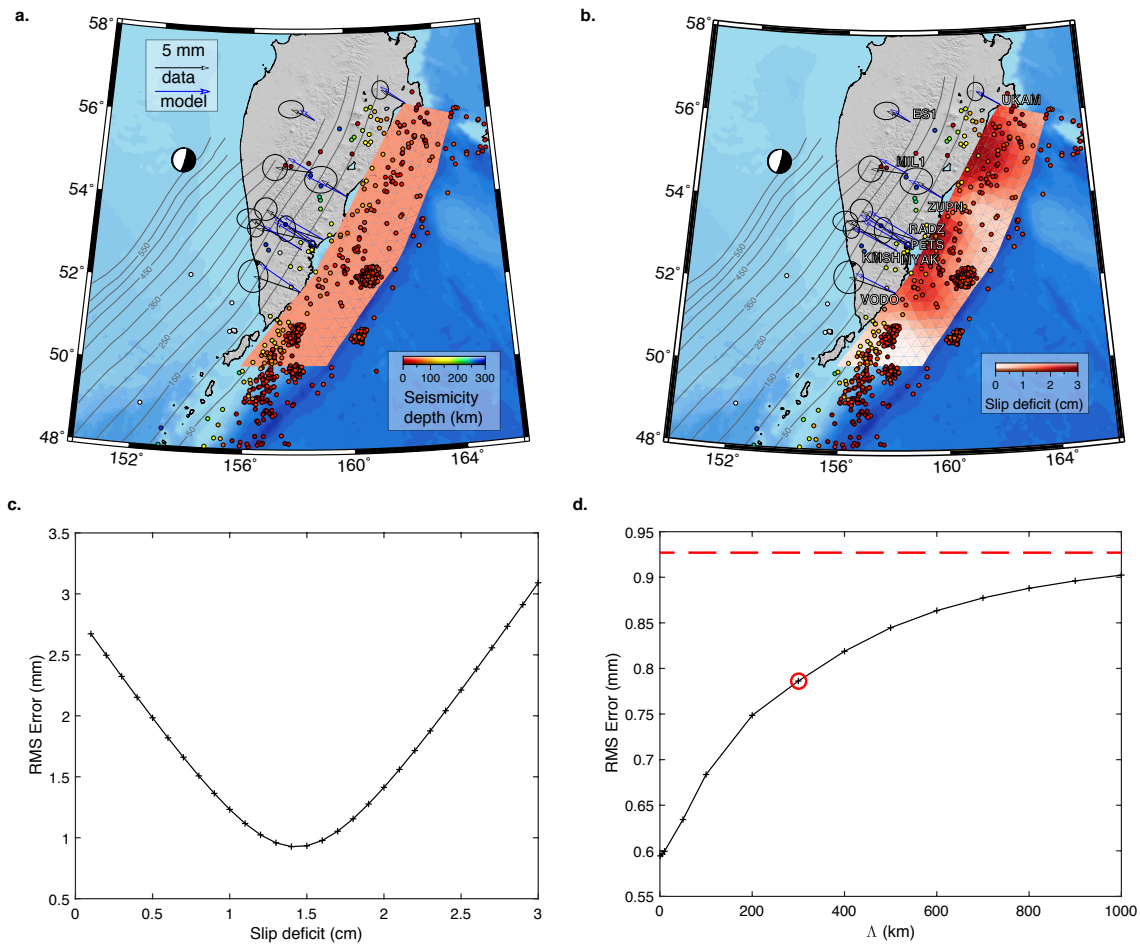
December 17, 2022, 1:47pm

Figure S8.   Model of slip deficit associated with the transient loading event. (a) Map of the best forward model with homogeneous slip deficit. The black arrows present the transient event static offsets and the blue arrows the associated modeled offsets. (b) Map of the inverse model corresponding to $\lambda = 300$ km. As in (a), black and blue arrows indicate the data and the model predictions. (c) RMS error versus slip deficit for the forward slip model of panel a. (d) RMS error as a function of the smoothing parameter λ for the slip deficit inverse models. The red circle correspond to the model presented in figure 4a and panel b. The red dashed line shows the minimum RMS error of panel c.
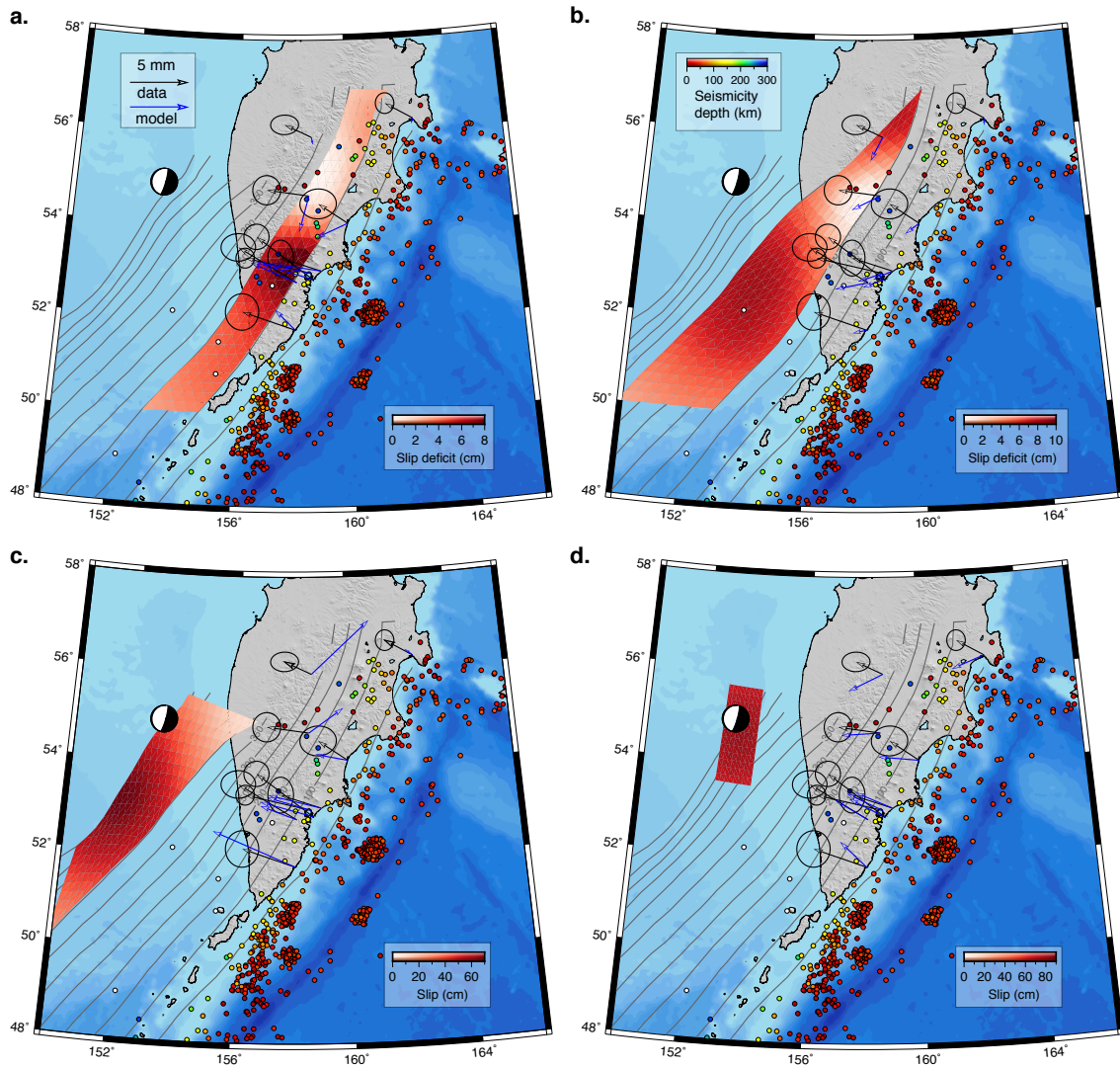
December 17, 2022, 1:47pm

Figure S9. **Inverse slip deficit and slip models tested for the April 2013 transient event.** (a and b) Slip deficit inverse models on the subduction interface for depths ranging from 100 to 200 km, and from 200 to 400 km respectively. The black arrows present the transient event static offsets and the blue arrows the associated modeled offsets. (c) Slip inverse model for depths ranging from 400 to 650 km. (d) Slip inverse model on the coseismic rupture plane modeled by (Ye et al., 2013)
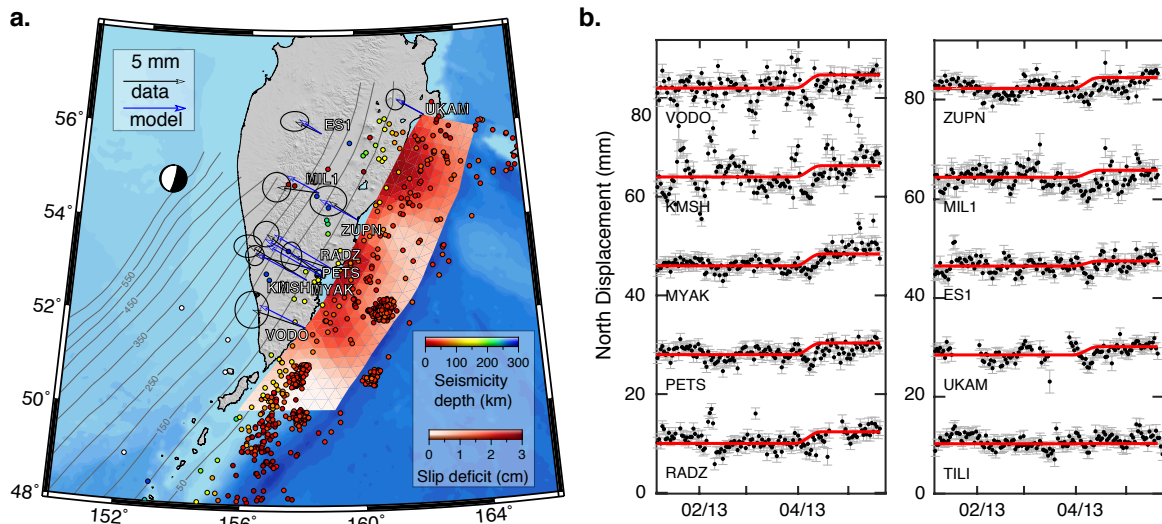
Figure S10.   **Seismogenic zone slip deficit inverse model of the transient loading event and fit to the north component time series.** (a) Map showing the static offsets of the transient loading event in black and the model predictions in blue. Slip deficit with amplitudes between 0 and 3 cm during a period of 18 days is shown with the red color-scale. Earthquakes that happened in 2013 before the Okhotsk earthquake are also shown, color-scaled by depth. (b) North GNSS position time series in black and model prediction time series in red.

December 17, 2022, 1:47pm